BNL-105160-2014-TECH

Booster Technical Note No. 116;BNL-105160-2014-IR

Booster beam loss due to beam-residual gas charge exchange

H. C. Hseuh

April 1988

Collider Accelerator Department

Brookhaven National Laboratory

U.S. Department of Energy

USDOE Office of Science (SC)

DISCLAIMER

BOOSTER BEAM LOSS

DUE TO BEAM-RESIDUAL GAS CHARGE EXCHANGE

AD

Booster Technical Note

No. 116

H. C. HSEUH

APRIL 20, 1988

ACCELERATOR DEVELOPMENT DEPARTMENT

Brookhaven National Laboratory

Upton, N.Y. 11973

BOOSTER BEAM LOSS DUE TO BEAM-RESIDUAL GAS CHARGE EXCHANGE

H.C. HSEUH

INTRODUCTION

The vacuum requirement of the Booster ring is mainly imposed by the interaction between the heavy ions and the residual gas molecules. Among the primary interactions, the cross sections of charge exchange (electron capture and strip) are several orders of magnitude higher than those of nuclear scattering and of multiple Coulomb scattering. The secondary interactions such as the secondary ion induced desorption, the bunch induced multipactoring and the beam neutralization are more relevant to storage rings than to the accelerators. The dominant beam loss process in the Booster, therefore, will be the charge exchange between the beam and the residual gas molecules.

The Booster vacuum requirement based on charge exchange was analyzed several years ago by G.R. Young (see RHIC-PG-16, December 8, 1983). In his note, a linac after Tandem was assumed, and there were only a few cross sectional data existed for extrapolation to Booster ranges. Since then, more abundant data are available, which make better estimate of the Booster vacuum requirement possible.

In this technical note, the best empirical formulae for charge exchange cross sections are selected. The beam losses due to charge exchanges are calculated for gold (Au+33) and iodine (I+29). At the designed vacuum of 3*10^-11 Torr (90% H_2 and 10% N_2/CO), the beam loss amounts to less than one percent for gold.

ELECTRON CAPTURE

The capture cross section can be expressed as

$$\sigma_{capt} \propto \beta^{\ell} * q^m * Zt^n$$

here $\beta = v/c$, q the projectile charge state, Zt the atomic number of the residual gas. The values of ℓ vary between -6 and -12, of m >= 2, and of n <= 1. The capture cross section is significant at low energy and drops off rapidly during the acceleration cycle.

Among the different experimental and theoretic works on predicting capture cross sections, the scaling rule proposed by A.S. Schlachter, et.al (Phys. Rev. A27, 3372(1983)) gives the best fitting to the existing data and is used in this note. A detailed comparison of several empirical formulae with the experimental data is given in Appendix.

ELECTRON LOSS(STRIP)

The loss cross sections can be expressed as

$$\sigma_{str} \propto \beta^{\ell} * q^{m} * Zt^{n} * Zp^{r}$$

with Zp the atomic number of the projectile (heavy ions).

Calculations of the loss cross sections based on plane wave Born approximation and inner shell ionizations are available in the literatures. At Booster energy range (β > 0.05), the loss cross sections decrease slowly with increasing β (with ℓ between -1 and -2) and become the dominant beam loss process at higher energy. A modified empirical formula based on Bohr-Lindhard formulae (H.D. Betz, Rev. MOd. Phys. 44, 465(1972)) is used in our calculation.

$$\sigma_{str} = 9*10^{-19}*q^{-3}*\beta^{-1}*Zt*Zp^{2} \qquad (1)$$

The results are within a factor of two of the existing data. Detailed comparison among different empirical formulae and the existing data is also given in Appendix.

BEAM LOSS DUE TO CHARGE EXCHANGE

The beam loss due to charge exchange can be expressed by

$$-dN/N = \sigma_t * n * dl \quad \text{or} \quad N/No = \exp\left(-\int_0^t \sigma_t * n * dl\right)$$

with -dN/N the fraction of the beam loss after travelling dl
σ_t the sum of the capture and the strip cross sections
n the gas density, = 3.3*10^16 * P
P pressure in Torr
dl the distance travelled, = $\beta * c * dt$

We know the charge states of the heavy ions from Tandem. The composition of the residual gas at certain pressures can be specified. Now we need $\beta(t)$ or E(t) to derive the cross sections.

Based on the acceleration schemes in the design manual, we have the equation for the energy gain for the ions as

$$dE(t) = V(t) * \sin\theta * q / A * \beta(t) * c / \phi * dt$$

with V(t) the peak RF voltage
θ the stable phase angle(between 17° and 22°)
A the atomic mass of the heavy ions
ϕ the circumferance of the ring.

The E(t) and $\beta(t)$ can be calculated by integrating dE(t) over t after injection and capture, then σ_t and N/No can be derived. This integration will be rather complicated and messy, since V, β, E and σ_t are functions of one another through the acceleration cycle. Instead, we have opted to calculate them through consecutive intervals with small increment in t, for example with dt = 1 msec.

Two cases are analyzed, Au +33 at 0.92 MeV/A (latest energy and charge state available from Tandem) and I+29 at 1.65 MeV/A.

The peak RF voltages V(t) are

Au+33 V = 0.88+0.69*t KV for t (= 20 ms and 14.6 KV for t) 20 ms
I+29 V = 0.64+0.64*t KV for t (= 20 ms and 13.5 KV for t) 20 ms

An average stable phase angle of 20 ^{o} is assumed.

The following vacuum conditions are specified:

3*10^-11 Torr - 90% H_2 and 10% CO (designed vacuum)
1*10^-10 Torr - 50% H_2 and 50% N_2 (due to small leaks)
3*10^-10 Torr - 90% N_2 and 10% H_2 (due to large leaks).

The calculation for gold over the first 50 ms is given in Table I. The "LOSS" and "SUM-L" are the instant and accumulated beam loss(in percent). For a mixture of gases, the cross section will be the fractional summing of the individual ones (i.e. CAPT1 = 0.9 * CAPT-H + 0.1 *CAPT-N).

The capture and loss(strip) cross sections for N_2/CO and for H_2 are plotted versus β in Figures 1 & 2 for Au and I respectively. On figures 3 and 4, the β and the accumulated beam loss at these three vacuum conditions are plotted against t for the first 500 msec. At the designed vacuum of 3*10^-11 Torr, the beam loss for all the heavy ions will be less than one percent. This agrees with Young's estimate.

At 3*10^-10 Torr, upto 30 % of gold would be lost while less than 10% of iodine would not survive. This results are higher than those of Young's, and are understandable, since we assumed 90% nitrogen which would be the worst case.

CONCLUSION

The Booster ring vauum requirement is analyzed based on the the charge exchange between beam and the residual gas molecules. The cross sections are estimated rather conservatively. The calculated beam loss is, therefore the upper bound. At the designed vacuum of 3*10^-11 Torr (90% hydrogen), the beam loss for the heaviest ions such as gold will be negligibly small.

The beam loss during the multiturn injection and before rf capture are not included here. It should be small because of the short period ((1ms). Slower rf capture and acceleration will lead to slightly higher loss rates.

APPENDIX. CHARGE EXCHANGE CROSS SECTIONS

The electron capture and loss cross sections considered here should include both single and multiple electron capture and loss. However multiple cross sections are usually less than 20% of the single cross section (H. Knudson et.al. Phys. Rev. A23, 597(1981) and W.G. Graham et.al. Phys. Rev. A30, 722(1984)) and can be

neglected for practical purpose.

The existing theoretical works and the experimental data cover a wide range of heavy ions, charge states, energy ranges and target gases. We will try to select some empirical or semi-empirical formulae, which give best fitting to the existing data.

CAPTURE CROSS SECTION

In general, the single electron capture cross sections are characterized by the ratio v/vo, with vo the Bohr velocity (= 2.2*10^8 cm/s). In the intermediate- and high-energy range(v/vo))1), the cross sections generally scale as v^-ℓ with ℓ approaching 11 at high . The cross sections also scale with q^m and Zt^n with m)2 and n)1.

Most of the theoretical works center on that of the Bohr-Lindhards' equation of

$$\sigma_{capt} = \pi * ao^2 * Zt^{1/3} * q^2 * (vo/v)^6$$

with ao the Bohr radius (=5.3*10^-9 cm). Three emphirical formulae as well as the "Scaling Rule" discussed below are selected to calculate the capture cross sections. They are compared with the experimental data in Table II.

Note that for diatomic gas, the predicted cross sections should be twice of those given by these equations.

SCALING RULE FOR CAPTURE CROSS SECTION

A universal scaling rule proposed by A.S. Schlachter et.al. (Phys. Rev. A27, 3372(1983) permits prediction of cross sections for a wide range of fast, highly charged heavy ions in different gas targets.

It uses the generalized reduced coordinates

$$\sigma' = \sigma_{capt} * Zt^{1.8} / q^{0.5} \quad \text{and} \quad E' = E / (Zt^{1.25} * q^{0.7})$$

then the capture cross sections σ can be calculated thru σ' by

$$\sigma' = \frac{1.1*10^{-8}*[1-\exp(0.037*E'^{2.2})][1-\exp(2.44*10^{-5}*E^{2.6})]}{E'^{4.8}}$$

As can be seen in Table II, it fits well to over 90% of the data (within a factor of two) with the exception of those for light ions and from ref. D.

LOSS(STRIP) CROSS SECTION

The most recent theoreical investigation of the strip cross sections are reported by G.H. Gillespie (Nucl. Instr. Methods, 176, 611(1980) using sum rules and by I.S. Dmitriev (Nucl. Instr.

Methods, 164, 329(1979) using a semiempirical formula. In their works, the Bethe inelastic scattering cross sections for individual initial and final states were summed up. The formulae show a strong β^{-2} dependent and can be expressed as

$$\sigma_{str} = 8\pi * a_o^2 * \alpha^2 * [\ I\ ] / \beta^2$$

with α the fine structure constant (= 0.0073), and I the collision strength.

These calculations include both the exitation (which does not necessarily lead to electron loss) and the ionization. They, therefore, usually overestimate the actual loss cross sections, sometimes by more than one order of magnitude. The formulae are better suited for low q, low Z ions with $\beta > 0.1$.

Several other semiempirical formulae obtained by fitting the experimental data to the model described in H.D. Betz. They have the following general form:

$$\sigma_{str} = A * \beta^{\ell} * q^m * Zt^n * Zp^r$$

with ℓ between -1 to -1.5, m -3 to -4, n < 2 and r 2 to 2.5. We have selected and modified that of J. Alonso and H. Gould (Phys. Rev. A26, 1134(1982)) for our calculation, which gives the best fit to the existing data.

Comparison among the different formulae is given in Table III. With the exception of those with "****", the formula of HCH gives within a factor of two to the experimental data. Most of those with "****" are again from ref. D. The calculated values from sum rules are also listed under "X-expt" from ref. G.

Note again for the diatomic gas, the calculated values should be multiplied by 2 to take into account the molecular effect.

TABLE I. CHARGE EXCHANGE CROSS SECTIONS AND BEAM LOSS IN BOOSTER
Au(+33, E_{inj} = 0.92 MeV/A)

beta' = [1-(1+E/931.5)^-2]^.5
W = beta*C/201.6 = 1490*beta turns/ms
V = 0.8+0.7*t KV (t (20 ms) or = 14.6KV
dE = W*V*sin(20)*33/197 = (0.068+0.06*t)*beta MeV/ms for t (20 ms
or 1.246*beta MeV/ms for t) 20 ms
E' = 1000*E/(Zt^1.25*Q^0.7) = 86.5*E(H) = 7.6*E(CO)
CAP' = 1.1e-8*[1-exp(-2.44e-5*E'^2.6)]/E'^4.8
CAP-H = 2*CAP'H*Q^0.5/Zt^1.8 = 11.4*CAP'H
CAP-CO = 2*CAP'CO*Q^0.5/Zt^1.8 = 0.346*CAP'CO
CAP1(90H) = CAP-H*0.9 + CAP-CO*0.1
CAP2(50H) = CAP-H*0.5 + CAP-CO*0.5
CAP3(10H) = CAP-H*0.1 + CAP-CO*0.9
TOTAL = CAP1 + STR1 or CPA2 + STR2 or CAP3 + STR3
LOSS = (-1/N)(dN/dt) = TOTAL*l*n n = 3.3*10^16*P(Torr)
= 9.9*10^23*beta*P*TOTAL /ms l = beta*C*dt

STR = 9e-19*Q^-3*beta^-1*Zt*Zp^2
STR-H = 2*STR = 3.1e-19/beta
STR-CO = 2*STR = 2.2e-18/beta
STR1(90H) = 0.9*STR-H + 0.1*STR-CO
STR2(50H) = 0.5*STR-H + 0.5*STR-CO
STR3(10H) = 0.1*STR-H + 0.9*STR-CO

LOSS = percent of beam loss over dt
SUM = cumulative beam loss from 0 to t

				X-SR E'				Capture Cross Section 90H 50H 10H					Strip Cross Section 90H 50H 10H			Pressure in Torr 3^-11		1^-10		3^-10	
t(ms	beta	beta'	E MeV/A	dE	E'H	E'CO	CAP-H	CAP-CO	CAP1	CAP2	CAP3	STR-H	STR-CO	STR1	STR2	STR3	LOSS	SUM	LOSS	SUM	LOSS	SUM
0		0.04	0.9		79.	6.9											0	0	0	0	0	0
1	0.04	0.04	0.9	0.00	80.	7.0	9E-17	1E-15	2E-16	7E-16	1E-15	7E-18	5E-17	1E-17	3E-17	5E-17	0.02	0.02	0.31	0.31	1.61	1.61
2	0.04	0.04	0.9	0.00	80.	7.0	8E-17	1E-15	2E-16	7E-16	1E-15	7E-18	5E-17	1E-17	3E-17	4E-17	0.02	0.05	0.31	0.63	1.59	3.18
3	0.04	0.04	0.9	0.01	81.	7.1	8E-17	1E-15	2E-16	7E-16	1E-15	7E-18	5E-17	1E-17	3E-17	4E-17	0.02	0.08	0.30	0.93	1.57	4.70
4	0.04	0.04	0.9	0.01	82.	7.2	8E-17	1E-15	2E-16	6E-16	1E-15	7E-18	5E-17	1E-17	3E-17	4E-17	0.02	0.11	0.30	1.23	1.54	6.18
5	0.04	0.04	0.9	0.01	84.	7.4	7E-17	1E-15	2E-16	6E-16	1E-15	7E-18	5E-17	1E-17	3E-17	4E-17	0.02	0.13	0.29	1.52	1.50	7.59
6	0.04	0.04	0.9	0.01	86.	7.5	7E-17	1E-15	2E-16	6E-16	1E-15	7E-18	5E-17	1E-17	3E-17	4E-17	0.02	0.16	0.28	1.81	1.46	8.94
7	0.04	0.04	1.0	0.02	88.	7.7	6E-17	1E-15	2E-16	6E-16	1E-15	7E-18	5E-17	1E-17	3E-17	4E-17	0.02	0.18	0.27	2.08	1.41	10.2
8	0.04	0.04	1.0	0.02	90.	7.9	6E-17	1E-15	2E-16	5E-16	9E-16	7E-18	5E-17	1E-17	3E-17	4E-17	0.02	0.21	0.26	2.34	1.36	11.4
9	0.04	0.04	1.0	0.02	92.	8.1	5E-17	1E-15	1E-16	5E-16	9E-16	6E-18	5E-17	1E-17	3E-17	4E-17	0.02	0.23	0.25	2.59	1.31	12.6
10	0.04	0.04	1.1	0.03	95.	8.3	4E-17	9E-16	1E-16	5E-16	8E-16	6E-18	5E-17	1E-17	3E-17	4E-17	0.02	0.25	0.24	2.82	1.25	13.7
11	0.04	0.04	1.1	0.03	98.	8.6	4E-17	9E-16	1E-16	4E-16	8E-16	6E-18	4E-17	1E-17	3E-17	4E-17	0.01	0.27	0.23	3.05	1.19	14.7
12	0.04	0.05	1.1	0.03	101	8.9	3E-17	8E-16	1E-16	4E-16	7E-16	6E-18	4E-17	1E-17	2E-17	4E-17	0.01	0.29	0.21	3.26	1.13	15.7
13	0.05	0.05	1.2	0.04	105	9.2	3E-17	7E-16	1E-16	4E-16	7E-16	6E-18	4E-17	1E-17	2E-17	4E-17	0.01	0.30	0.20	3.46	1.07	16.8
14	0.05	0.05	1.2	0.04	109	9.6	2E-17	7E-16	9E-17	4E-16	6E-16	6E-18	4E-17	1E-17	2E-17	4E-17	0.01	0.32	0.19	3.65	1.01	17.4
15	0.05	0.05	1.3	0.05	114	10.	2E-17	6E-16	8E-17	3E-16	6E-16	6E-18	4E-17	9E-18	2E-17	4E-17	0.01	0.33	0.18	3.82	0.95	18.2
16	0.05	0.05	1.3	0.05	118	10.	2E-17	6E-16	7E-17	3E-16	5E-16	6E-18	4E-17	9E-18	2E-17	4E-17	0.01	0.35	0.17	3.99	0.89	18.9
17	0.05	0.05	1.4	0.05	123	10.	1E-17	5E-16	7E-17	3E-16	5E-16	6E-18	4E-17	9E-18	2E-17	4E-17	0.01	0.36	0.16	4.14	0.83	19.8
18	0.05	0.05	1.4	0.06	129	11.	1E-17	5E-16	6E-17	2E-16	4E-16	5E-18	4E-17	9E-18	2E-17	4E-17	0.01	0.37	0.14	4.29	0.78	20.2
19	0.05	0.05	1.5	0.06	135	11.	9E-18	4E-16	5E-17	2E-16	4E-16	5E-18	4E-17	9E-18	2E-17	3E-17	0.01	0.38	0.13	4.42	0.73	20.8
20	0.05	0.05	1.6	0.07	141	12.	8E-18	4E-16	5E-17	2E-16	4E-16	5E-18	4E-17	8E-18	2E-17	3E-17	0.00	0.39	0.12	4.54	0.68	21.4
21	0.05	0.06	1.7	0.07	147	13.	6E-18	4E-16	4E-17	2E-16	3E-16	5E-18	4E-17	8E-18	2E-17	3E-17	0.00	0.40	0.12	4.66	0.63	21.9
22	0.06	0.06	1.7	0.07	154	13.	5E-18	3E-16	4E-17	2E-16	3E-16	5E-18	4E-17	8E-18	2E-17	3E-17	0.00	0.41	0.11	4.77	0.59	22.3
23	0.06	0.06	1.8	0.07	161	14.	4E-18	3E-16	3E-17	2E-16	3E-16	5E-18	3E-17	8E-18	2E-17	3E-17	0.00	0.41	0.10	4.87	0.55	22.8
24	0.06	0.06	1.9	0.07	167	14.	3E-18	3E-16	3E-17	1E-16	2E-16	5E-18	3E-17	8E-18	2E-17	3E-17	0.00	0.42	0.09	4.96	0.51	23.3
25	0.06	0.06	2.0	0.08	174	15.	3E-18	2E-16	3E-17	1E-16	2E-16	5E-18	3E-17	8E-18	2E-17	3E-17	0.00	0.43	0.09	5.05	0.48	23.5
26	0.06	0.06	2.1	0.08	182	15.	2E-18	2E-16	2E-17	1E-16	2E-16	5E-18	3E-17	7E-18	2E-17	3E-17	0.00	0.43	0.08	5.13	0.45	23.9
27	0.06	0.06	2.1	0.08	189	16.	2E-18	2E-16	2E-17	1E-16	2E-16	5E-18	3E-17	7E-18	2E-17	3E-17	0.00	0.44	0.08	5.21	0.43	24.2
28	0.06	0.06	2.2	0.08	196	17.	2E-18	2E-16	2E-17	9E-17	2E-16	4E-18	3E-17	7E-18	2E-17	3E-17	0.00	0.44	0.07	5.28	0.40	24.5
29	0.06	0.07	2.3	0.08	204	17.	1E-18	2E-16	2E-17	9E-17	2E-16	4E-18	3E-17	7E-18	2E-17	3E-17	0.00	0.45	0.07	5.35	0.38	24.8
30	0.07	0.07	2.4	0.08	211	18.	1E-18	2E-16	2E-17	8E-17	1E-16	4E-18	3E-17	7E-18	2E-17	3E-17	0.00	0.45	0.06	5.42	0.36	25.1
31	0.07	0.07	2.5	0.09	219	19.	9E-19	1E-16	2E-17	7E-17	1E-16	4E-18	3E-17	7E-18	2E-17	3E-17	0.00	0.46	0.06	5.48	0.34	25.3
32	0.07	0.07	2.6	0.09	227	19.	7E-19	1E-16	1E-17	7E-17	1E-16	4E-18	3E-17	7E-18	2E-17	3E-17	0.00	0.46	0.05	5.54	0.32	25.6
33	0.07	0.07	2.7	0.09	235	20.	6E-19	1E-16	1E-17	6E-17	1E-16	4E-18	3E-17	7E-18	2E-17	3E-17	0.00	0.47	0.05	5.59	0.31	25.8
34	0.07	0.07	2.8	0.09	243	21.	5E-19	1E-16	1E-17	6E-17	1E-16	4E-18	3E-17	6E-18	2E-17	3E-17	0.00	0.47	0.05	5.64	0.29	26.0
35	0.07	0.07	2.9	0.09	252	22.	5E-19	1E-16	1E-17	5E-17	1E-16	4E-18	3E-17	6E-18	2E-17	3E-17	0.00	0.48	0.05	5.70	0.28	26.3
36	0.07	0.08	3.0	0.09	260	22.	4E-19	1E-16	1E-17	5E-17	9E-17	4E-18	3E-17	6E-18	2E-17	3E-17	0.00	0.48	0.05	5.74	0.26	26.4
37	0.08	0.08	3.1	0.09	269	23.	3E-19	9E-17	9E-18	5E-17	8E-17	4E-18	3E-17	6E-18	2E-17	2E-17	0.00	0.48	0.04	5.79	0.25	26.6
38	0.08	0.08	3.2	0.10	278	24.	3E-19	8E-17	9E-18	4E-17	8E-17	4E-18	3E-17	6E-18	2E-17	2E-17	0.00	0.49	0.04	5.83	0.24	26.8
39	0.08	0.08	3.3	0.10	287	25.	2E-19	8E-17	8E-18	4E-17	7E-17	4E-18	3E-17	6E-18	1E-17	2E-17	0.00	0.49	0.04	5.88	0.23	27.0
40	0.08	0.08	3.4	0.10	296	26.	2E-19	7E-17	7E-18	4E-17	7E-17	4E-18	3E-17	6E-18	1E-17	2E-17	0.00	0.49	0.04	5.92	0.22	27.2
41	0.08	0.08	3.5	0.10	305	26.	2E-19	7E-17	7E-18	3E-17	6E-17	4E-18	3E-17	6E-18	1E-17	2E-17	0.00	0.50	0.04	5.96	0.21	27.3
42	0.08	0.08	3.6	0.10	314	27.	2E-19	6E-17	6E-18	3E-17	6E-17	4E-18	2E-17	6E-18	1E-17	2E-17	0.00	0.50	0.03	5.99	0.20	27.5
43	0.08	0.08	3.7	0.10	324	28.	1E-19	6E-17	6E-18	3E-17	5E-17	3E-18	2E-17	6E-18	1E-17	2E-17	0.00	0.50	0.03	6.03	0.19	27.6
44	0.08	0.09	3.8	0.11	333	29.	1E-19	5E-17	6E-18	3E-17	5E-17	3E-18	2E-17	5E-18	1E-17	2E-17	0.00	0.51	0.03	6.06	0.19	27.7
45	0.09	0.09	3.9	0.11	343	30.	1E-19	5E-17	5E-18	3E-17	5E-17	3E-18	2E-17	5E-18	1E-17	2E-17	0.00	0.51	0.03	6.10	0.18	27.9
46	0.09	0.09	4.0	0.11	353	31.	9E-20	5E-17	5E-18	2E-17	4E-17	3E-18	2E-17	5E-18	1E-17	2E-17	0.00	0.51	0.03	6.13	0.17	28.0
47	0.09	0.09	4.2	0.11	363	31.	8E-20	4E-17	4E-18	2E-17	4E-17	3E-18	2E-17	5E-18	1E-17	2E-17	0.00	0.52	0.03	6.16	0.17	28.1
48	0.09	0.09	4.3	0.11	373	32.	7E-20	4E-17	4E-18	2E-17	4E-17	3E-18	2E-17	5E-18	1E-17	2E-17	0.00	0.52	0.03	6.19	0.16	28.2
49	0.09	0.09	4.4	0.11	384	33.	6E-20	4E-17	4E-18	2E-17	3E-17	3E-18	2E-17	5E-18	1E-17	2E-17	0.00	0.52	0.03	6.22	0.15	28.4
50	0.09	0.09	4.5	0.12	394	34.	5E-20	4E-17	4E-18	2E-17	3E-17	3E-18	2E-17	5E-18	1E-17	2E-17	0.00	0.52	0.02	6.25	0.15	28.5

TABLE II

COMPARISON OF THE ELECTRON CAPTURE CROSS SECTIONS OF HEAVY IONS
from EXPERIMENTAL DATA AND EMPIRICAL FORMULAE

SR X =1.1e-8*q^0.5*(1-exp(-2.44e-5*E'^2.6))/(E'^4.8*Zt^1.8)
w/ E'=1000*E/(Zt^1.25*q^0.7)
BL X =3.14*(5.3e-9)^2*Zt^0.33*q^2*(vo/v)^6
HJH X =1e-28*q^2.5*Zt^0.67*beta^-7
VSN X =4*3.14*(5.3e-9)^2*Zt^0.33*q^3*(vo/v)^6

P	q	Zt	Beta	E MeV/A	Xexpt	ref.	E'	X-SR		X-BL	X-HJH	X-VSN
C	5	2	0.067	2.098	8.4E-20	A	285.	1.1E-20	***	4.8E-21	1.5E-18	9.7E-20
C	6	1	0.025	0.31	6.2E-17	F	88.4	1.1E-17	***	1.7E-18	1.2E-15	4.2E-17
C	6	1	0.049	1.14	1.7E-19	F	325.	2.4E-20	***	3.4E-20	1.2E-17	8.3E-19
C	6	2	0.025	0.31	1.3E-16	F	37.1	5.7E-17		2.2E-18	1.9E-15	5.3E-17
C	6	2	0.049	1.14	1.0E-18	F	136.	4.3E-19		4.3E-20	2.0E-17	1.0E-18
C	6	10	0.049	1.14	1.7E-17	F	18.2	1.7E-17		7.3E-20	5.7E-17	1.8E-18
C	6	18	0.049	1.14	3.3E-17	F	8.77	3.0E-17		8.8E-20	8.5E-17	2.2E-18
N	7	2	0.062	1.796	2.5E-19	A	193.	8.9E-20	***	1.5E-20	5.9E-18	4.3E-19
O	8	2	0.073	2.492	8.6E-20	A	244.	3.1E-20		7.3E-21	2.6E-18	2.4E-19
F	9	2	0.073	2.492	1.4E-19	A	225.	4.8E-20		9.2E-21	3.5E-18	3.4E-19
Ar	13	7	0.084	3.35	5.3E-18	E	48.8	4.2E-18		1.2E-20	7.3E-18	6.4E-19
Ar	14	7	0.084	3.35	6.3E-18	E	46.3	5.1E-18		1.4E-20	8.8E-18	8.0E-19
Ar	15	7	0.084	3.35	1.2E-17	E	44.1	6.0E-18		1.6E-20	1.0E-17	9.9E-19
Ar	16	7	0.084	3.35	1.5E-17	E	42.2	7.0E-18		1.8E-20	1.2E-17	1.2E-18
Ar	17	7	0.084	3.35	1.4E-17	E	40.4	8.1E-18		2.1E-20	1.4E-17	1.4E-18
Ar	18	7	0.084	3.35	1.7E-17	E	38.9	9.3E-18		2.3E-20	1.6E-17	1.7E-18
Ar	13	7	0.111	5.8	8.0E-19	E	84.5	6.2E-19		2.4E-21	1.1E-18	1.3E-19
Ar	14	7	0.111	5.8	1.5E-18	E	80.3	7.9E-19		2.7E-21	1.3E-18	1.6E-19
Ar	15	7	0.111	5.8	1.6E-18	E	76.5	1.0E-18		3.1E-21	1.5E-18	1.9E-19
Ar	16	7	0.111	5.8	3.0E-18	E	73.1	1.2E-18		3.6E-21	1.8E-18	2.3E-19
Ar	17	7	0.111	5.8	3.3E-18	E	70.1	1.5E-18		4.0E-21	2.1E-18	2.8E-19
Ar	18	7	0.111	5.8	4.8E-18	E	67.3	1.8E-18		4.5E-21	2.4E-18	3.3E-19
Ar	13	7	0.123	7.1	4.6E-19	E	103.	2.5E-19		1.3E-21	5.3E-19	6.8E-20
Ar	15	7	0.123	7.1	1.1E-18	E	93.6	4.2E-19		1.7E-21	7.5E-19	1.0E-19
Ar	14	7	0.134	8.5	2.3E-19	E	117.	1.4E-19		8.8E-22	3.5E-19	5.0E-20
Ar	15	7	0.134	8.5	4.8E-19	E	112.	1.8E-19		1.0E-21	4.1E-19	6.2E-20
Ar	16	7	0.134	8.5	5.4E-19	E	107.	2.4E-19		1.2E-21	4.9E-19	7.5E-20
Ar	17	7	0.134	8.5	8.0E-19	E	102.	3.0E-19		1.3E-21	5.7E-19	9.0E-20
Ar	18	7	0.134	8.5	1.0E-18	B	98.7	3.7E-19		1.5E-21	6.5E-19	1.1E-19
Ar	16	18	0.084	3.4	2.3E-17	F	13.1	2.0E-17		2.5E-20	2.3E-17	1.6E-18
Ar	17	18	0.134	8.5	2.4E-18	F	31.5	2.8E-18		1.8E-21	1.1E-18	1.2E-19
Ar	18	18	0.134	8.5	2.4E-18	F	30.3	3.2E-18		2.0E-21	1.2E-18	1.5E-19
Fe	17	7	0.134	8.5	9.1E-19	E	102.	3.0E-19		1.3E-21	5.7E-19	9.0E-20
Fe	20	7	0.134	8.5	1.1E-18	E	91.6	5.4E-19		1.8E-21	8.5E-19	1.5E-19
Fe	23	7	0.134	8.5	2.3E-18	E	83.1	8.8E-19		2.4E-21	1.2E-18	2.2E-19
Fe	25	7	0.134	8.5	2.7E-18	E	78.4	1.2E-18		2.8E-21	1.5E-18	2.9E-19
Fe	26	7	0.134	8.5	3.4E-18	E	76.3	1.3E-18		3.0E-21	1.6E-18	3.2E-19
Fe	20	18	0.047	1.07	1.5E-16	F	3.54	4.1E-16		1.2E-18	2.2E-15	9.7E-17
Fe	21	18	0.047	1.07	1.4E-16	F	3.42	4.5E-16		1.3E-18	2.5E-15	1.1E-16
Fe	23	18	0.085	3.4	3.9E-17	F	10.2	4.2E-17		4.9E-20	5.4E-17	4.6E-18
Fe	24	18	0.085	3.4	4.3E-17	F	9.91	4.6E-17		5.4E-20	6.0E-17	5.3E-18
Fe	25	18	0.085	3.4	4.5E-17	F	9.63	5.0E-17		5.8E-20	6.6E-17	5.9E-18
Fe	25	18	0.134	8.4	5.7E-18	F	23.8	6.6E-18		3.8E-21	2.8E-18	3.9E-19
Fe	26	18	0.134	8.4	6.0E-18	F	23.1	7.2E-18		4.2E-21	3.1E-18	4.4E-19
Kr	21	7	0.134	8.5	4.5E-19	F	88.6	6.4E-19		2.0E-21	9.6E-19	1.7E-19
Kr	27	7	0.134	8.5	2.2E-18	E	74.3	1.5E-18		3.3E-21	1.8E-18	3.6E-19
Kr	33	7	0.134	8.5	6.6E-18	E	64.5	2.8E-18		4.9E-21	3.0E-18	6.6E-19
Nb	28	1	0.085	3.4	1.0E-19	F	329.	4.7E-20		2.8E-20	1.3E-17	3.2E-18
Nb	31	1	0.085	3.4	1.2E-19	F	307.	7.0E-20		3.4E-20	1.6E-17	4.4E-18
Nb	34	1	0.085	3.4	2.1E-19	F	288.	1.0E-19		4.1E-20	2.1E-17	5.8E-18
Nb	31	18	0.085	3.4	6.0E-17	F	8.28	7.8E-17		8.9E-20	1.1E-16	1.1E-17
Xe	34	7	0.134	8.5	3.7E-18	E	63.2	3.0E-18		5.2E-21	3.2E-18	7.2E-19
Xe	41	7	0.134	8.5	7.7E-18	E	55.4	5.1E-18		7.6E-21	5.1E-18	1.3E-18
Xe	46	7	0.134	8.5	1.2E-17	E	51.1	6.9E-18		9.5E-21	6.8E-18	1.8E-18
Xe	32	7	0.134	8.5	4.5E-18	C	65.9	2.5E-18		4.6E-21	2.8E-18	6.0E-19

TABLE II(conti.)

P	q	Zt	Beta	E MeV/A	Xexpt	ref.	E'	X-SR		X-BL	X-HJH	X-VSN
Pb	51	1	0.099	4.66	3.1E-19	F	297.	1.1E-19		3.7E-20	1.9E-17	7.6E-18
Pb	52	1	0.099	4.66	3.2E-19	F	293.	1.1E-19		3.8E-20	2.0E-17	8.1E-18
Pb	53	1	0.099	4.66	3.3E-19	F	289.	1.2E-19		3.9E-20	2.1E-17	8.5E-18
Pb	54	1	0.099	4.66	3.8E-19	F	285.	1.3E-19		4.1E-20	2.2E-17	9.0E-18
Pb	55	1	0.099	4.66	3.9E-19	F	281.	1.4E-19		4.2E-20	2.3E-17	9.5E-18
Pb	56	1	0.099	4.66	4.6E-19	F	278.	1.5E-19		4.4E-20	2.4E-17	1.0E-17
Pb	57	1	0.099	4.66	4.8E-19	F	274.	1.6E-19		4.6E-20	2.5E-17	1.1E-17
Pb	58	1	0.099	4.66	4.4E-19	F	271.	1.7E-19		4.7E-20	2.6E-17	1.1E-17
Pb	59	1	0.099	4.66	4.6E-19	F	268.	1.9E-19		4.9E-20	2.7E-17	1.2E-17
Pb	54	2	0.099	4.66	8.9E-19	F	120.	2.4E-18	***	5.1E-20	3.5E-17	1.1E-17
Pb	37	7	0.099	4.66	3.0E-17	C	32.6	2.1E-17		3.7E-20	3.2E-17	5.5E-18
Pb	40	7	0.099	4.66	4.0E-17	C	30.9	2.5E-17		4.3E-20	3.8E-17	7.0E-18
Pb	52	7	0.099	4.66	9.0E-17	C	25.7	4.3E-17		7.2E-20	7.4E-17	1.5E-17
Pb	37	7	0.134	8.5	6.5E-18	C	59.6	3.9E-18		6.2E-21	4.0E-18	9.3E-19
Pb	40	7	0.134	8.5	7.0E-18	C	56.4	4.8E-18		7.2E-21	4.8E-18	1.2E-18
Pb	52	7	0.134	8.5	1.0E-17	C	46.9	9.4E-18		1.2E-20	9.3E-18	2.6E-18
Pb	40	7	0.112	5.9	1.3E-17	D	39.1	1.4E-17		2.1E-20	1.7E-17	3.5E-18
Pb	54	7	0.099	4.66	8.8E-17	F	25.0	4.7E-17		7.8E-20	8.1E-17	1.7E-17
Pb	55	7	0.112	5.9	2.2E-17	D	31.3	2.8E-17		4.0E-20	3.7E-17	9.0E-18
Pb	54	10	0.099	4.66	4.8E-17	F	16.0	6.8E-17		8.7E-20	1.0E-16	1.9E-17
Pb	54	18	0.099	4.66	8.3E-17	F	7.70	1.2E-16		1.1E-19	1.5E-16	2.3E-17
Pb	54	54	0.099	4.66	7.5E-17	F	1.95	3.5E-16	***	1.5E-19	3.2E-16	3.4E-17
U	14	1	0.054	1.4	6.0E-19	D	220.	2.3E-19		1.0E-19	5.0E-17	5.7E-18
U	20	1	0.054	1.4	1.0E-18	D	171.	9.2E-19		2.0E-19	1.2E-16	1.7E-17
U	30	1	0.054	1.4	4.0E-18	D	129.	4.4E-18		4.6E-19	3.4E-16	5.6E-17
U	40	1	0.128	7.8	1.2E-18	D	589.	3.5E-21	***	4.8E-21	1.7E-18	7.9E-19
U	63	1	0.145	10	3.6E-19	D	550.	6.1E-21	***	5.8E-21	2.3E-18	1.5E-18
U	10	7	0.054	1.4	1.0E-18	D	24.5	2.1E-17	***	9.7E-20	7.9E-17	4.0E-18
U	20	7	0.054	1.4	2.0E-17	D	15.1	9.1E-17	***	3.9E-19	4.5E-16	3.2E-17
U	30	7	0.054	1.4	1.2E-16	D	11.3	2.1E-16		8.7E-19	1.2E-15	1.1E-16
U	63	7	0.145	10	1.6E-17	D	48.3	9.6E-18		1.1E-20	8.5E-18	2.8E-18

*** more than a factor of two difference between X-expt and X-SR
X-SR = A.S. Schlachter, et.al., Phys. Rev. A27, 3372 (1983).
X-BL = N. Bohr & J. Lindhard, K. Dan Vidensk. Selsk. Mat. Fys. Medd. 28, 7 (1954).
or H.D. Betz, Rev. Mod. Pyhs. 44, 465(1972)
X-HJH = D. Blechschmidt & H.J. Halama, Proc. 1977 Heavy Ion Fusion Workshop, p136.
X-VSN = V.S. Nikolaev, et.al., J. Phys. B8, 158 (1975).

References for experimental data:
A = T.R. Dillingham, et. al., Phys. Rev. A24, 1237 (1981).
B = H. Gould, et. al., Phys. Rev. Lett, 41, 1457 (1978).
C = J. Alonso and H. Gould, Phys. Rev. A26, 1134 (1982).
D = B. Franzke, IEEE Trans. Nucl. Sci. NS-28, 2116 (1981).
E = J. Alonso, et. al., IEEE Trans. Nucl. Sci. NS-26, 3686 (1979).
F = W.G. Graham, et. al., Phys. Rev. A30, 722 (1984).
and Phys. Rev. A17, 1284 (1978).

TABLE III

COMPARISON OF ELECTRON LOSS CROSS SECTIONS OF HEAVY IONS
from EXPERIMENTAL WORKS and EMPIRICAL FORMULAE

BL X = 3.14*(5.3e-9)^2*Zt^0.67*Zp^1.33*q^-3*(vo/v)^2
HCH X = 9e-19*q^-3*beta^-1*Zt*Zp^2
JA X = 1e-19*q^-3*beta^-1.5*Zp^2*Zt
JA1 X = 5e-19*q^-2*beta^-1*Zp^1.33*Zt

P	Zp	q	Zt	Beta	E MeV/A	X-expt	Ref.	X-HCH		X-JA	X-JA1	X-BL
Ar	18	13	7	0.0845	3.35	8.6E-18	E	1.1E-17		4.2E-18	1.1E-17	5.2E-18
Ar	18	14	7	0.0845	3.35	4.3E-18	E	8.8E-18		3.4E-18	9.9E-18	4.1E-18
Ar	18	15	7	0.0845	3.35	2.3E-18	E	7.2E-18	***	2.7E-18	8.6E-18	3.4E-18
Ar	18	13	7	0.111	5.8	6.6E-18	E	8.4E-18		2.8E-18	8.7E-18	3.0E-18
Ar	18	14	7	0.111	5.8	4.6E-18	E	6.7E-18		2.2E-18	7.5E-18	2.4E-18
Ar	18	15	7	0.111	5.8	2.2E-18	E	5.4E-18		1.8E-18	6.5E-18	1.9E-18
Ar	18	13	7	0.123	7.1	5.7E-18	E	7.6E-18		2.4E-18	7.9E-18	2.4E-18
Ar	18	15	7	0.123	7.1	2.3E-18	E	4.9E-18		1.6E-18	5.9E-18	1.6E-18
Ar	18	13	7	0.134	8.5	5.2E-18	E	6.9E-18		2.1E-18	7.2E-18	2.1E-18
Ar	18	14	7	0.134	8.5	3.1E-18	E	5.6E-18		1.7E-18	6.2E-18	1.6E-18
Ar	18	15	7	0.134	8.5	1.8E-18	E	4.5E-18	***	1.4E-18	5.4E-18	1.3E-18
Ar	18	16	7	0.134	8.5	4.3E-18	E	3.7E-18		1.1E-18	4.8E-18	1.1E-18
Ar	18	17	7	0.134	8.5	3.7E-18	E	3.1E-18		9.4E-19	4.2E-18	9.2E-19
Ar	18	17	18	0.134	8.5	2.5E-18	F	8.0E-18	***	2.4E-18	1.1E-17	1.7E-18
Fe	26	17	7	0.134	8.5	8.2E-18	E	6.5E-18		2.0E-18	6.9E-18	1.5E-18
Fe	26	20	7	0.134	8.5	4.1E-18	E	4.0E-18		1.2E-18	5.0E-18	9.2E-19
Fe	26	23	7	0.134	8.5	8.0E-19	E	2.6E-18	***	7.9E-19	3.8E-18	6.0E-19
Fe	26	25	7	0.134	8.5	3.2E-19	E	2.0E-18	***	6.2E-19	3.2E-18	4.7E-19
Kr	36	21	7	0.134	8.5	9.4E-18	E	6.6E-18		2.0E-18	7.0E-18	1.2E-18
Kr	36	27	7	0.134	8.5	1.8E-18	E	3.1E-18		9.4E-19	4.2E-18	5.8E-19
Kr	36	33	7	0.134	8.5	2.3E-19	E	1.7E-18	***	5.1E-19	2.8E-18	3.2E-19
Nb	41	28	1	0.0852	3.4	3.2E-19	F	8.1E-19	***	3.1E-19	1.0E-18	4.1E-19
Nb	41	31	1	0.0852	3.4	2.2E-19	F	6.0E-19		2.3E-19	8.5E-19	3.0E-19
Nb	41	34	1	0.0852	3.4	4.0E-20	F	4.5E-19	***	1.7E-19	7.1E-19	2.3E-19
Nb	41	31	18	0.0852	3.4	1.2E-18	F	1.1E-17	***	4.1E-18	1.5E-17	2.1E-18
Xe	54	20	1	0.447	110	9.0E-19	G	7.3E-19		1.2E-19	5.6E-19	5.9E-20
Xe	54	30	1	0.447	110	4.0E-19	G	2.2E-19		3.6E-20	2.5E-19	1.8E-20
Xe	54	40	1	0.447	110	1.5E-19	G	9.2E-20		1.5E-20	1.4E-19	7.4E-21
Xe	54	10	7	0.447	110	2.2E-17	G	4.1E-17		6.8E-18	1.6E-17	1.7E-18
Xe	54	20	7	0.447	110	1.2E-17	G	5.1E-18		8.5E-19	3.9E-18	2.2E-19
Xe	54	30	7	0.447	110	6.0E-18	G	1.5E-18		2.5E-19	1.8E-18	6.5E-20
Xe	54	40	7	0.447	110	2.0E-18	G	6.4E-19		1.1E-19	9.9E-19	2.7E-20
Xe	54	28	7	0.134	8.5	1.8E-17	E	6.2E-18		1.9E-18	6.7E-18	8.8E-19
Xe	54	34	7	0.134	8.5	5.3E-18	E	3.5E-18		1.1E-18	4.6E-18	4.9E-19
Xe	54	41	7	0.134	8.5	1.6E-18	E	2.0E-18		6.0E-19	3.1E-18	2.8E-19
Xe	54	32	7	0.134	8.5	4.5E-18	C	4.2E-18		1.3E-18	5.1E-18	5.9E-19
Hg	80	10	7	0.447	110	1.7E-17	G	9.0E-17	***	1.5E-17	2.7E-17	2.9E-18
Hg	80	20	7	0.447	110	9.2E-18	G	1.1E-17		1.9E-18	6.6E-18	3.7E-19
Hg	80	34	7	0.447	110	5.6E-18	G	2.3E-18		3.8E-19	2.3E-18	7.5E-20
Hg	80	52	7	0.447	110	1.5E-18	G	6.4E-19		1.1E-19	9.8E-19	2.1E-20
Pb	82	51	1	0.0996	4.66	4.3E-19	F	4.6E-19		1.6E-19	6.8E-19	1.3E-19
Pb	82	52	1	0.0996	4.66	3.5E-19	F	4.3E-19		1.5E-19	6.5E-19	1.2E-19
Pb	82	53	1	0.0996	4.66	3.4E-19	F	4.1E-19		1.4E-19	6.3E-19	1.1E-19
Pb	82	54	1	0.0996	4.66	2.5E-19	F	3.9E-19		1.4E-19	6.0E-19	1.1E-19
Pb	82	55	1	0.0996	4.66	2.3E-19	F	3.7E-19		1.3E-19	5.8E-19	1.0E-19
Pb	82	56	1	0.0996	4.66	2.1E-19	F	3.5E-19		1.2E-19	5.6E-19	9.5E-20
Pb	82	57	1	0.0996	4.66	1.8E-19	F	3.3E-19		1.2E-19	5.4E-19	9.0E-20
Pb	82	58	1	0.0996	4.66	1.4E-19	F	3.1E-19		1.1E-19	5.2E-19	8.5E-20
Pb	82	59	1	0.0996	4.66	1.4E-19	F	3.0E-19		1.0E-19	5.1E-19	8.1E-20
Pb	82	54	2	0.0996	4.66	2.8E-19	F	7.7E-19	***	2.7E-19	1.2E-18	1.7E-19
Pb	82	37	7	0.0996	4.66	2.0E-17	C	8.4E-18		3.0E-18	9.0E-18	1.2E-18
Pb	82	40	7	0.0996	4.66	1.5E-17	C	6.6E-18		2.3E-18	7.7E-18	9.6E-19
Pb	82	52	7	0.0996	4.66	3.0E-18	C	3.0E-18		1.1E-18	4.6E-18	4.4E-19
Pb	82	37	7	0.134	8.5	1.0E-17	C	6.2E-18		1.9E-18	6.7E-18	6.7E-19
Pb	82	40	7	0.134	8.5	1.0E-17	C	4.9E-18		1.5E-18	5.7E-18	5.3E-19
Pb	82	40	7	0.112	5.9	1.6E-17	D	5.9E-18		2.0E-18	6.9E-18	7.6E-19
Pb	82	52	7	0.134	8.5	3.0E-18	C	2.2E-18		6.8E-19	3.4E-18	2.4E-19
Pb	82	54	7	0.0996	4.66	3.2E-18	F	2.7E-18		9.5E-19	4.2E-18	3.9E-19
Pb	82	55	7	0.112	5.9	6.6E-18	D	2.3E-18		7.5E-19	3.6E-18	2.9E-19
Pb	82	54	10	0.0996	4.66	1.8E-18	F	3.9E-18		1.4E-18	6.0E-18	4.9E-19
Pb	82	54	18	0.0996	4.66	2.5E-18	F	6.9E-18	***	2.4E-18	1.1E-17	7.3E-19
Pb	82	54	54	0.0996	4.66	3.9E-18	F	2.1E-17	***	7.3E-18	3.3E-17	1.5E-18

TABLE III(conti.)

P	Zp	q	Zt	Beta	E MeV/A	X-expt	Ref.	X-HCH		X-JA	X-JA1	X-BL
U	92	10	1	0.0547	1.4	3.0E-17	D	1.4E-16	***	6.6E-17	3.7E-17	6.4E-17
U	92	14	1	0.0547	1.4	1.3E-17	D	5.1E-17	***	2.4E-17	1.9E-17	2.3E-17
U	92	20	1	0.0547	1.4	7.0E-18	D	1.7E-17	***	8.3E-18	9.3E-18	8.0E-18
U	92	30	1	0.0547	1.4	1.3E-18	D	5.2E-18	***	2.5E-18	4.2E-18	2.4E-18
U	92	40	1	0.1286	7.8	1.0E-19	D	9.3E-19	***	2.9E-19	9.9E-19	1.8E-19
U	92	63	1	0.0547	10	1.6E-19	D	5.6E-19	***	2.6E-19	9.4E-19	2.6E-19
U	92	10	7	0.0547	1.4	4.0E-16	D	9.7E-16		4.6E-16	2.6E-16	2.4E-16
U	92	20	7	0.0547	1.4	4.0E-17	D	1.2E-16	***	5.8E-17	6.5E-17	3.0E-17
U	92	30	7	0.0547	1.4	1.2E-17	D	3.6E-17	***	1.7E-17	2.9E-17	8.8E-18
U	92	30	7	0.0547	1.4	3.0E-17	D	3.6E-17		1.7E-17	2.9E-17	8.8E-18
U	92	63	7	0.1453	10	8.0E-18	D	1.5E-18		4.3E-19	2.5E-18	1.3E-19
U	92	40	18	0.0547	1.4	8.0E-18	D	3.9E-17	***	1.9E-17	4.2E-17	7.0E-18
U	92	50	18	0.0547	1.4	1.3E-18	D	2.0E-17	***	9.5E-18	2.7E-17	3.6E-18
U	92	10	1	0.447	110	3.0E-18	G	1.7E-17	***	2.8E-18	4.6E-18	9.6E-19
U	92	20	1	0.447	110	1.5E-18	G	2.1E-18		3.5E-19	1.1E-18	1.2E-19
U	92	30	1	0.447	110	1.0E-18	G	6.3E-19		1.0E-19	5.1E-19	3.6E-20
U	92	40	1	0.447	110	6.5E-19	G	2.7E-19		4.4E-20	2.9E-19	1.5E-20
U	92	50	1	0.447	110	4.5E-19	G	1.4E-19		2.3E-20	1.8E-19	7.7E-21
U	92	10	7	0.447	110	4.0E-17	G	1.2E-16	***	2.0E-17	3.2E-17	3.5E-18
U	92	20	7	0.447	110	2.5E-17	G	1.5E-17		2.5E-18	8.0E-18	4.4E-19
U	92	30	7	0.447	110	1.7E-17	G	4.4E-18		7.3E-19	3.6E-18	1.3E-19
U	92	40	7	0.447	110	1.1E-17	G	1.9E-18	***	3.1E-19	2.0E-18	5.5E-20
U	92	50	7	0.447	110	7.0E-18	G	9.5E-19	***	1.6E-19	1.3E-18	2.8E-20

References for experimental data:
A = T.R. Dillingham, et. al., Phys. Rev. A24, 1237 (1981).
B = H. Gould, et. al., Phys. Rev. Lett, 41, 1457 (1978).
C = J. Alonso and H. Gould, Phys. Rev. A26, 1134 (1982).
D = B. Franzke, IEEE Trans. Nucl. Sci. NS-28, 2116 (1981).
E = J. Alonso, et. al., IEEE Trans. Nucl. Sci. NS-26, 3686 (1979).
F = W.G. Graham, et. al., Phys. Rev. A30, 722 (1984).
G = Calculations by G.H. Gillespie using "Sum Rules"
G.H. Gillespie, et. al., Proc. Heavy Ion Fusion Workshop, 1977 & 1978.
and Phys. Rev. A17, 1284 (1978).

*** more than a factor of two difference between X-expt and X-HCH
X-HCH = best fitting based on the following three references.
X-BL = N. Bohr & J. Lindhard, K. Dan Vidensk. Selsk. Mat. Fys. Medd. 28, 7 (1954).
or H.D. Betz, Rev. Mod. Phys. 44, 465(1972).
X-JA = J. Alonso & H. Gould, Phys. Rev. A26, 1134(1982).
X-JA1 = Modification to X-JA.

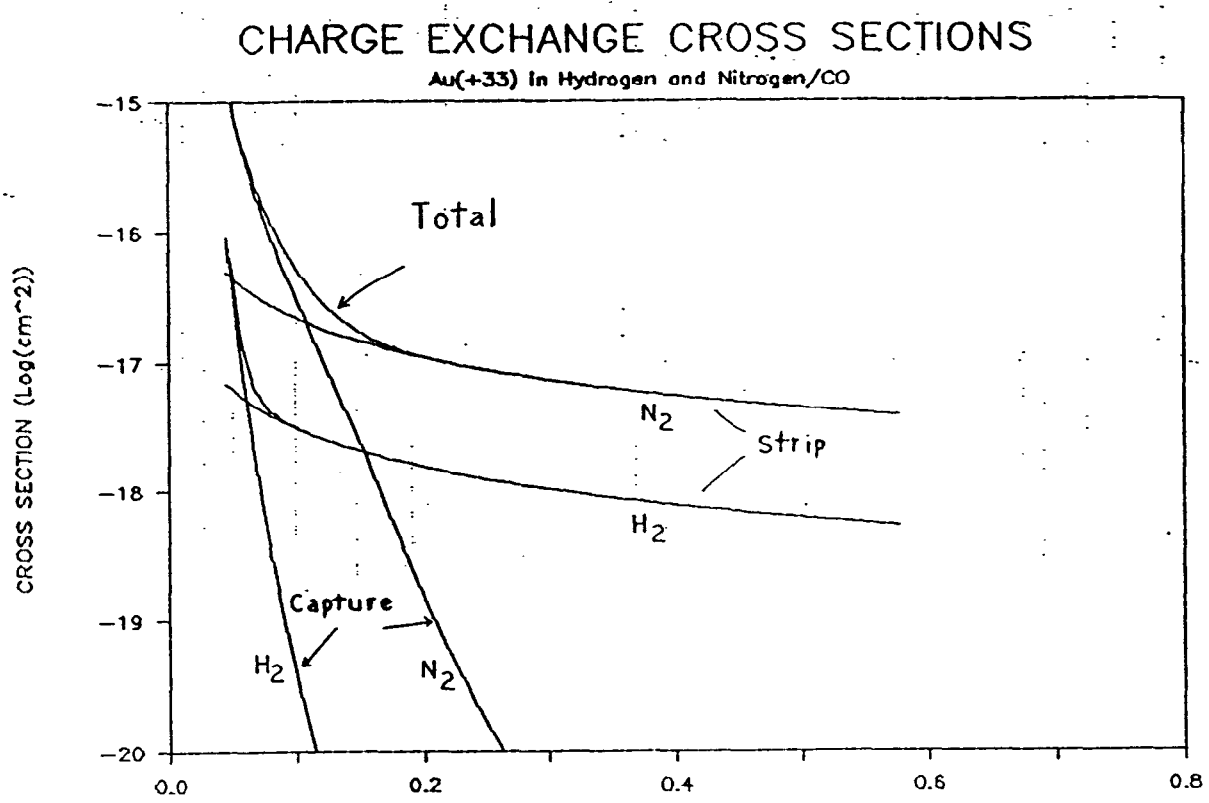
CHARGE EXCHANGE CROSS SECTIONS
Au(+33) in Hydrogen and Nitrogen/CO
CROSS SECTION (Log(cm^2))
-15
-16
-17
-18
-19
-20
0.0
0.2
0.4
0.6
0.8
Beta = v/c
Total
N2
Strip
H2
Capture
H2
N2

Fig. 1.

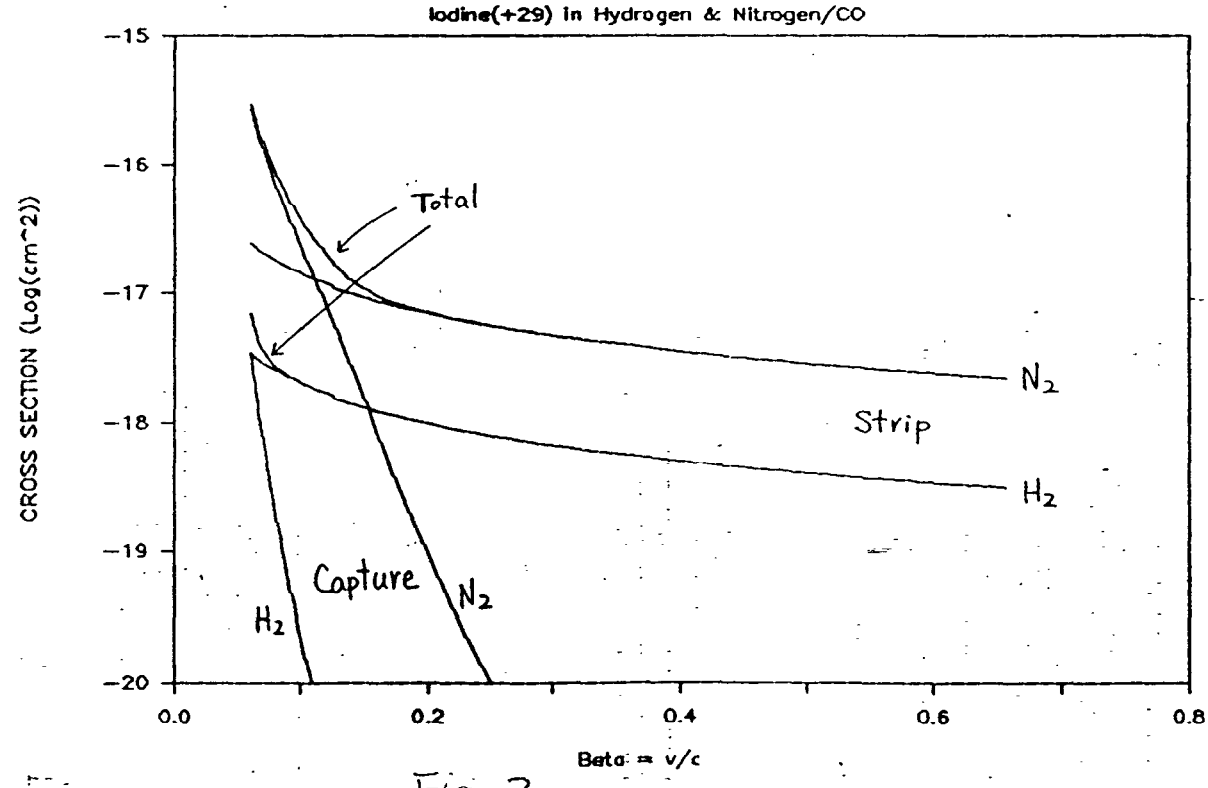
Iodine(+29) in Hydrogen & Nitrogen/CO
CROSS SECTION (Log(cm^2))
-15
-16
-17
-18
-19
-20
0.0
0.2
0.4
0.6
0.8
Beta = v/c
Total
N2
Strip
H2
Capture
H2
N2

Fig. 2.

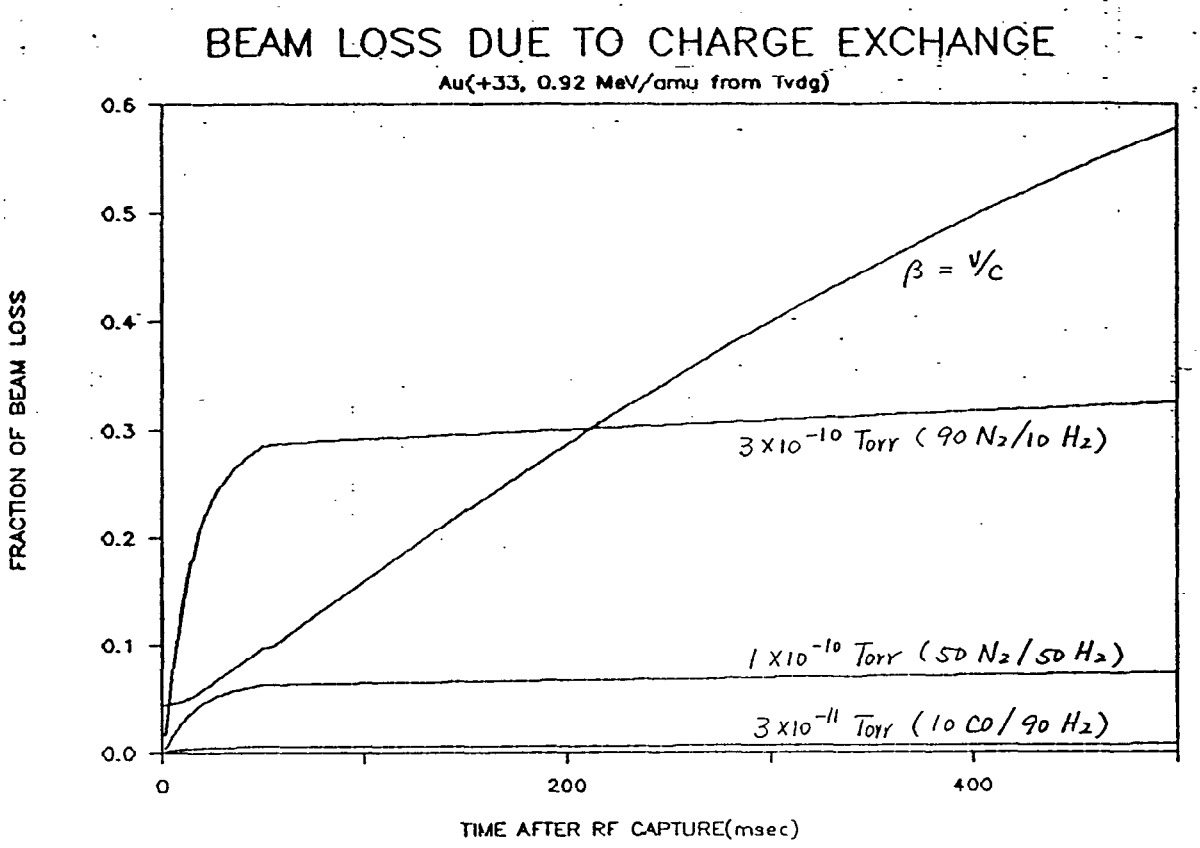
BEAM LOSS DUE TO CHARGE EXCHANGE
Au(+33, 0.92 MeV/amu from Tvdg)
FRACTION OF BEAM LOSS
0.0
0.1
0.2
0.3
0.4
0.5
0.6
0
200
400
TIME AFTER RF CAPTURE(msec)
β = v/c
3 X10⁻¹⁰ Torr (90 N₂/10 H₂)
1 X10⁻¹⁰ Torr (50 N₂/50 H₂)
3 X10⁻¹¹ Torr (10 CO/90 H₂)

Fig. 3.

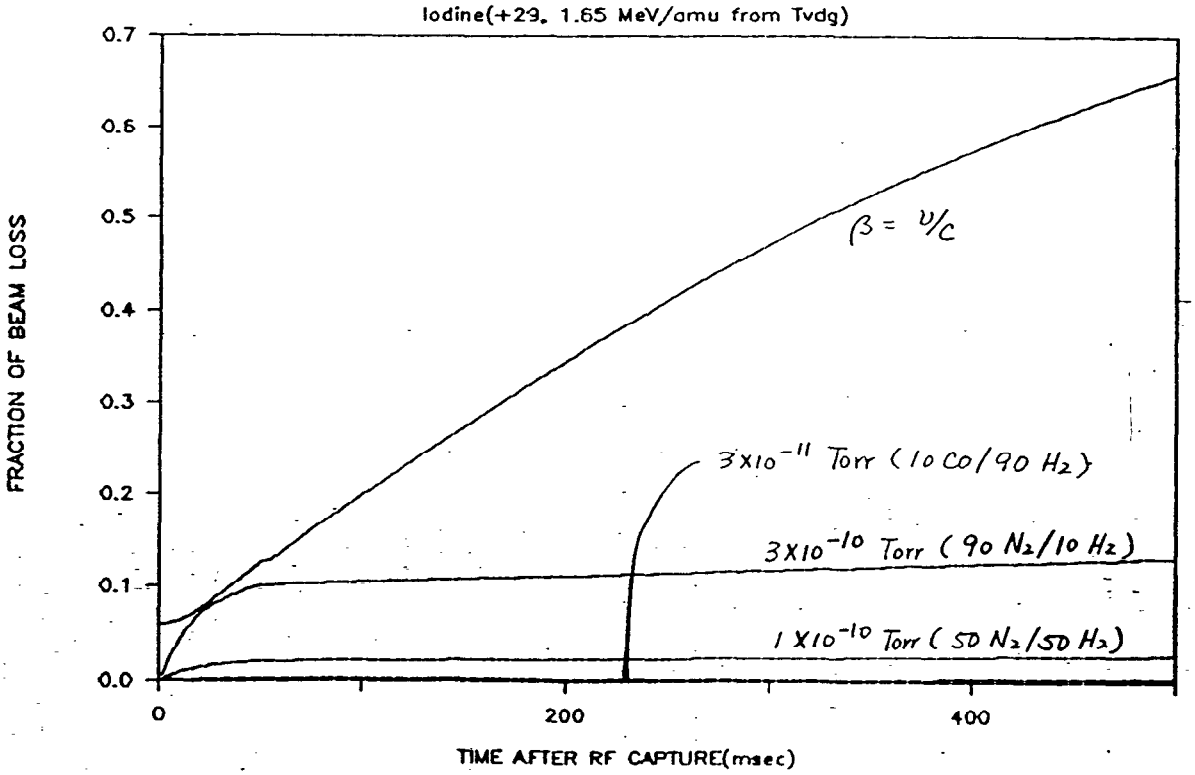
Iodine(+29, 1.65 MeV/amu from Tvdg)
FRACTION OF BEAM LOSS
0.0
0.1
0.2
0.3
0.4
0.5
0.6
0.7
0
200
400
TIME AFTER RF CAPTURE(msec)
β = v/c
3X10⁻¹¹ Torr (10 CO/90 H₂)
3X10⁻¹⁰ Torr (90 N₂/10 H₂)
1 X10⁻¹⁰ Torr (50 N₂/50 H₂)

Fig 4.